medRxiv preprint doi: https://doi.org/10.1101/2022.05.16.22275130; this version posted June 15, 2022. The copyright holder for this preprint (which was not certified by peer review) is the author/funder, who has granted medRxiv a license to display the preprint in perpetuity. It is made available under a CC-BY-NC 4.0 International license .

Modelling long-term COVID-19 hospital admission dynamics using immune protection waning data

Bastien Reyné[1*], Mircea T. Sofonea[1=], Samuel Alizon[1,2=]

1 MIVEGEC, Univ. Montpellier, CNRS, IRD — Montpellier, France
2 CIRB, College de France, CNRS, INSERM, Université PSL — Paris, France

* corresponding author : bastien.reyne@ird.fr
= equal contribution

Abstract

Immune waning is key to the timely anticipation of COVID-19 long-term dynamics. We assess the impact of periodic vaccination campaigns using a compartmental epidemiological model with multiple age structures and parameterised using empiric time-dependent vaccine protection data. Despite the uncertainty inherent to such scenarios, we show that vaccination campaigns decreases the yearly number of COVID-19 admissions. However, especially if restricted to individuals over 60 years old, vaccination on its own seems insufficient to prevent thousands of hospital admissions and it suffers the comparison with non-pharmaceutical interventions aimed at decreasing infection transmission. The combination of such interventions and vaccination campaigns appear to provide the greatest reduction in hospital admissions.

1 Introduction

From the beginning, Covid-19 pandemic management had to deal with numerous unknowns and strongly relied on mathematical modelling to guide non-pharmaceutical interventions (NPIs) implementation. The rapid discovery of efficient vaccines led to the hope that public health policy planning could soon return to normal. However, long-term forecasts are difficult because vaccine protection decreases with time [UKHSA, 2022]. Furthermore, the emergence of variants of concerns (VOC) raises major concerns, especially because of lineages from the Omicron variant (Pango lineage BA) that exhibit strong immune escape properties.

In the French context, Bosetti et alii, 2022, studied under what booster administration and NPIs implementation a new epidemic could be contained. However, their work was done before the Omicron VOC, and only on a six-month horizon. Kissler et alii, 2020 investigated the potential long-term effects of the seasonality observed in other epidemics than that of SARS-CoV-2. They highlighted the need for NPIs, but their results were obtained before vaccine implementation and the emergence of VOCs. Saad-Roy et alii, 2021 studied different vaccine administration patterns for several scenarios of immunity duration but, their long-term insights were very uncertain because at the time, there was no data on immune protection waning. Finally, Ghosh et alii [2022] used a non-Markovian setting to capture immunity waning but remain on a few months horizon.

The waning of immune protection is challenging to capture with classical compartmental models because it implies an exponential increase in the number of model compartments, which makes precise parameterization challenging. We extend a non-Markovian approach [Reyné et alii, 2022] that readily accounts for the time spent in each compartment. By using published data, we explore long-term epidemic dynamics in a qualitative way. In our scenarios, we account for immunity waning as well as Omicron-specific phenotypic traits and compare four vaccination campaign strategies. Furthermore, we also investigate the impact of non-pharmaceutical interventions (NPIs), such as mask-wearing or air quality improvement, that can decrease the transmission rate of the infection.

NOTE: This preprint reports new research that has not been certified by peer review and should not be used to guide clinical practice.

medRxiv preprint doi: https://doi.org/10.1101/2022.05.16.22275130; this version posted June 15, 2022. The copyright holder for this preprint (which was not certified by peer review) is the author/funder, who has granted medRxiv a license to display the preprint in perpetuity. It is made available under a CC-BY-NC 4.0 International license .

2 Methods

An epidemiological model with time structures

We use an epidemiological compartmental model (Figure 1A) in which susceptible individuals of age a (the density of which is denoted S_a) can either become fully vaccinated (V_a), or contract a mild (I_a^m) or severe infection (I_a^s). Mildly-infected individuals always recover and move to the compartment R_a. Both recovered and vaccinated individuals can be (re)infected, but at a reduced rate compared to susceptible individuals. If this (re)infection is mild, individuals move to a separate compartment (I_a^{mv}) to account for a potential immunity-induced reduction in infectiousness. Vaccinated and recovered individuals may be (re)vaccinated and move to the booster compartment (B_a), where their protection increases. Finally, severely infected (I_a^s) and previously immunised mildly infected individuals (I_a^{mv}) also end up in the booster compartment upon recovery, assuming high protection against potential new infection. Overall, the boosted compartment consists of individuals with booster vaccination dose(s), two natural infections, one vaccination and one infection, or having recovered from a severe infection.

The model accounts for memory effects, meaning that we record the time spent by the individuals in each compartment. Knowing the time since vaccination (k) for vaccinated individuals, the time since clearance (j) for recovered individuals, and the time since the entry into the booster compartment (l), allows us to readily account for the waning in immune protection.

This model is based on a system of partial differential equations (Appendix S2). Its parameterization reflects the French epidemic and the Omicron VOC (Table 1) [Sofonea et alii, 2022].

Contact rates were allowed to vary with time and fitted using the hospital admissions time series up to May 6, 2022. Following a parsimony principle, we used the last fitted value as the baseline until the rest of the simulations.

External factors, such as the weather, are known to impact transmission dynamics [Ma et alii, 2021]. We included this seasonality by assuming sinusoidal variations such that in summer the contact rate is decreased to –10% and increased by +10% in the winter.

Immune waning

In contrast to earlier models, we could calibrate immunity waning using epidemiological data UKHSA [2022]. More precisely, we used time series of vaccine protection (whether initial doses or boosters) against both symptomatic disease and hospitalisation, for both Delta and Omicron VOC. We fitted linear models on the different time series (Figure 1B).

Vaccination campaign scenarios

Vaccinated individuals were assumed to receive a booster dose 6 months after entering the vaccinated (V_a) compartment. Then, we investigate four different scenarios:

Table 1: **Description of the Omicron-related model parameters and their default value.** For each parameter, we indicate the default value used, the range in the sensitivity analyses, and the references.

Parameter	Value retained	Range for SA	Reference
Omicron generation time	Gamma(1.84, 0.53)	See Appendix S3	UKSHA [2022]
Omicron VOC decrease in virulence	0.33	Not included	Nyberg et alii [2022]
Seasonality	0.1	$[0 - 0.2]$	Ma et alii [2021]
Vaccine efficacy	See Appendix S3	$+/-5\%$	UKHSA [2022]
Transmission reduction	0.5	$[0.45 - 0.55]$	Bosetti et alii [2022]

medRxiv preprint doi: https://doi.org/10.1101/2022.05.16.22275130; this version posted June 15, 2022. The copyright holder for this preprint (which was not certified by peer review) is the author/funder, who has granted medRxiv a license to display the preprint in perpetuity. It is made available under a CC-BY-NC 4.0 International license .

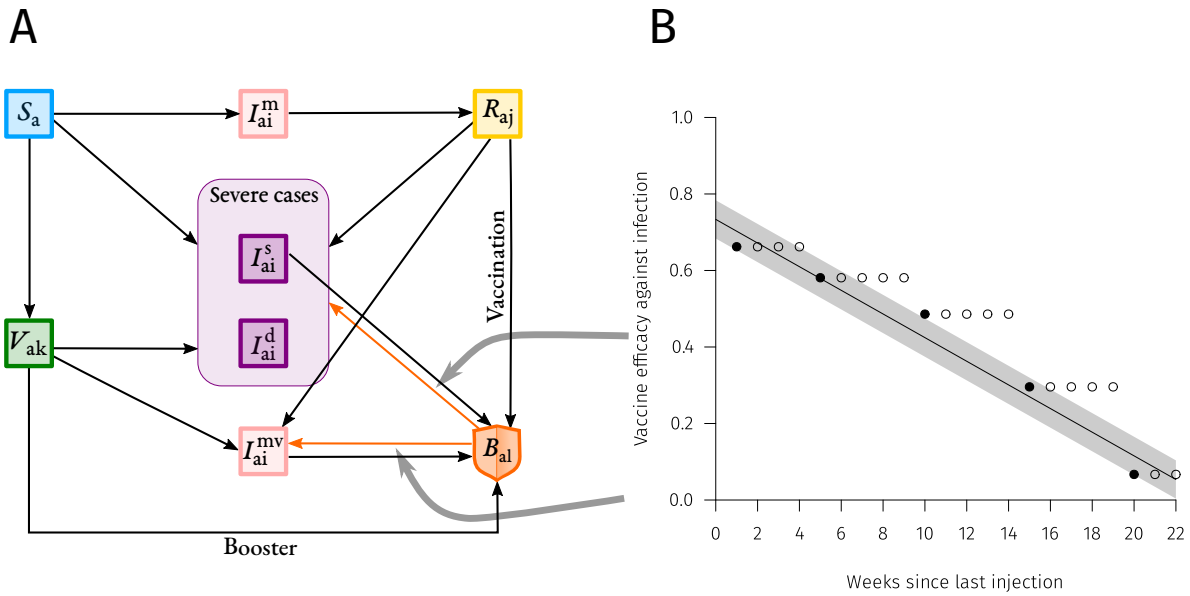

Figure 1: **Description of the memory-based model with immune waning. A)** Flowchart of the compartmental model. Arrows show transitions between compartments. S_a stands for Susceptible individuals of age a, I^m_{ai}, I^s_{ai}, I^d_{ai} and I^{mv}_{ai} stand respectively for mildly/severely/severely-that-will-die/mildly-partly-immune infected individuals of age a infected since i days, V_{ak} stands for Vaccinated individuals of age a vaccinated k days ago, R_{aj} stands for Recovered individuals of age a that cleared the disease j days ago and finally $B_{a\ell}$ stands for individuals of age a that received a booster vaccine dose ℓ days ago. Orange arrows show some of the transitions that depend on the time spent in the compartment (here ℓ days) that are parametrized through real immune waning data shown on panel B. **B)** Waning of vaccine efficacy against infection. Dots corresponds to real data from UKHSA [2022] for the Pfizer/BioNTech vaccine (BNT162b2) after a booster dose. The lines correspond to the baseline of the immunity decrease model implementation and the shaded areas to the uncertainty used within the sensitivity analysis. Here, we show the protection against an Omicron/BA.1 VOC infection for individuals that received a booster dose. Large grey arrows indicate where the waning data shown acts in the compartmental model.

medRxiv preprint doi: https://doi.org/10.1101/2022.05.16.22275130; this version posted June 15, 2022. The copyright holder for this preprint (which was not certified by peer review) is the author/funder, who has granted medRxiv a license to display the preprint in perpetuity. It is made available under a CC-BY-NC 4.0 International license .

- In Scenario A, boosted individuals are not vaccinated again.
- Scenario B consists in implementing annual vaccination campaigns before winter (in September and October) but only for individuals above 60 years old.
- We extend the yearly vaccination campaign to all the population in Scenario C.
- Scenario D assumes two national vaccine campaigns per year (in September – October and in March – April) for all the population.

To better assess the impact of vaccination campaigns, we also investigated two additional scenarios in which we implemented a decreased contact rate of -20% compared to the May 2022 value used in the baseline scenario. This value was chosen because it is comparable to others observed in 2021 [Reyné et alii, 2022].

3 Results

Scenario A leads to a high level of daily hospital admissions (Figure 2A) with yearly oscillations attributable to seasonality. Scenario B improves the overall situation but the median number of hospital admissions always remains above 500 per day (Figure 2B). Vaccinating everyone once a year (Scenario C) further lowers the number of daily hospital admissions and it also yields an epidemic wave in the early spring (Figure 2C). Finally, the fourth scenario (Figure 2D).lowers the number of daily hospital admissions even further but it does not prevent two marked epidemic waves per year.

Both Scenarios C and D have the more pronounced epidemic waves. This can be explained by the fact that vaccinating everyone at the same time implies that immunity wane for everyone at the same time.

Figure 2E shows the annual total number of hospital admissions for each scenario. As expected, the more the people are vaccinated, the more the daily hospital admissions lower. However, vaccination alone just seems to contain what was reached with stringent NPIs in 2021 in France (curfews, lockdown, health pass).

Note that, as shown also in Supplementary Figures S1 to S4, simulations yield large 95% confidence intervals (CI) for the total number of hospital admissions.

Finally, we also explored the impact of a 20% reductiong in the contact rate baseline for scenarios A and C (Supplementary Figures S5-S6). On its own the reduction in contact rate can have a stronger impact than yearly vaccination campaigns for the whole population (scenario A' in Figure 2E). Combining yearly vaccination and a decrease in contact rate provides the strongest decrease in the total number of yearly hospital admissions.

medRxiv preprint doi: https://doi.org/10.1101/2022.05.16.22275130; this version posted June 15, 2022. The copyright holder for this preprint (which was not certified by peer review) is the author/funder, who has granted medRxiv a license to display the preprint in perpetuity. It is made available under a CC-BY-NC 4.0 International license .

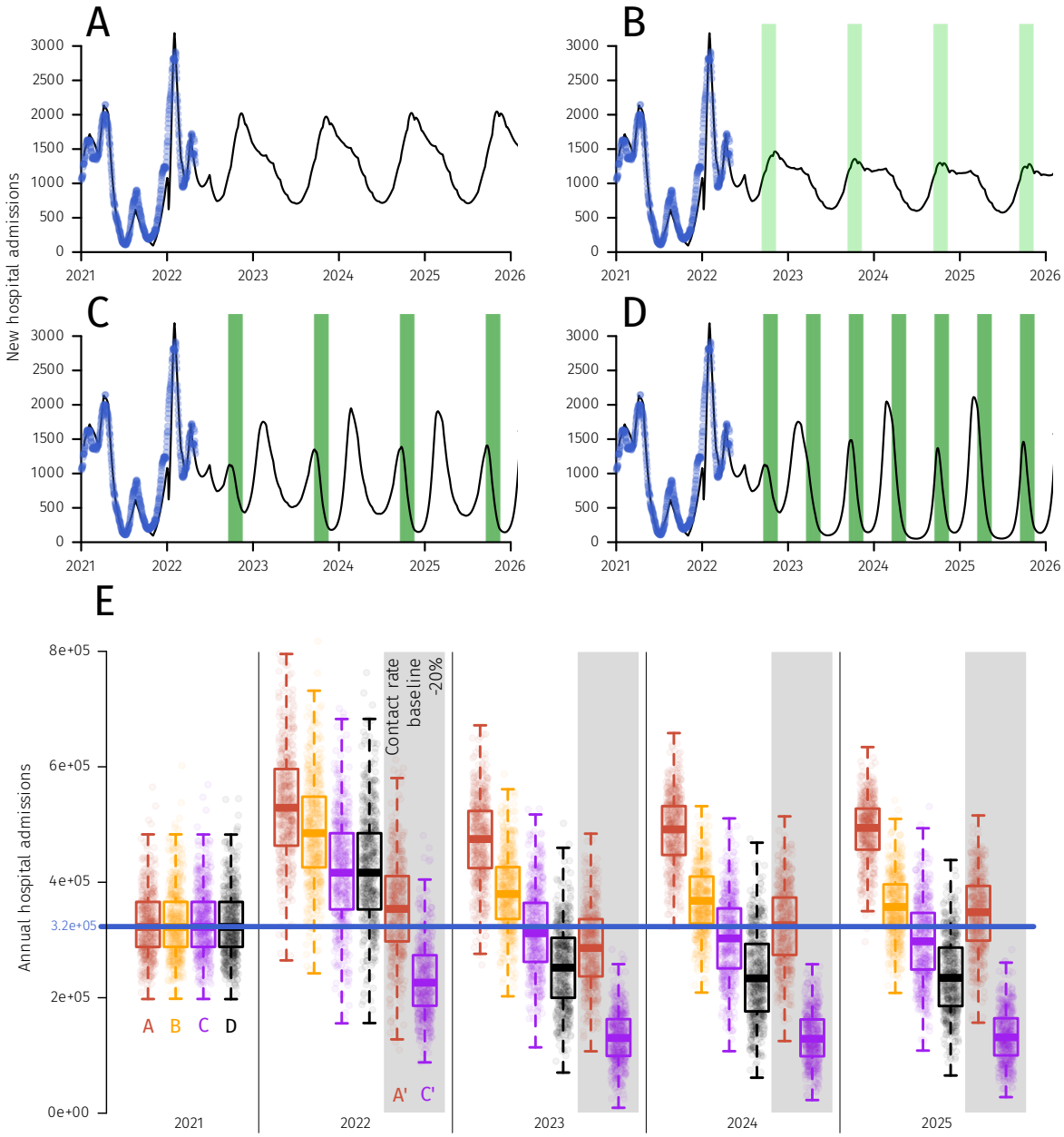

Figure 2: **Median number of COVID-19 hospital admissions in four vaccination campaign scenarios.** Blue dots corresponds to real data and green shaded areas to vaccination campaigns periods. The four panels correspond to scenarios without additional booster **(A)**, with an annual vaccination campaign in September-October for every individuals above 60 y.o. **(B)**, an annual vaccination campaign in September-October for the whole population **(C)**, and bi-annual vaccination campaign for the whole population **(D)** (in September-October and in March-April). See Supplementary Figures S1 to S4 for the 95% confidence intervals and the interquartile range. The panel **(E)** shows a comparison of the total number of hospital admissions per year for four vaccination scenarios. Blue line corresponds to real data for 2021. The different type of boxplots correspond to the different scenarios. Scenarios **A'** and **C'**, in the gray shaded area, corresponds to Scenarios A and C where the baseline contact rate was decreased by 20%. Complete dynamics for those alternate scenarios are shown in Supplementary Figures S5-S6.

medRxiv preprint doi: https://doi.org/10.1101/2022.05.16.22275130; this version posted June 15, 2022. The copyright holder for this preprint (which was not certified by peer review) is the author/funder, who has granted medRxiv a license to display the preprint in perpetuity. It is made available under a CC-BY-NC 4.0 International license .

4 Discussion

COVID-19 management now faces the challenge of post-infection and post-vaccination immune waning combined with the emergence risk of new VOCs.

Long term scenarios are obviously extremely uncertain but they can provide valuable insights. By leaning on Omicron-based data on immune protection, we show that immune waning may cause yearly epidemic hospitalization peaks comparable to the largest one seen in 2021. Although vaccination clearly mitigates this impact, it seems insufficient to suppress the epidemic. As shown in the Supplementary Figures S5-S6, variations in these contact rates, i.e. the intensity of NPIs or behavourial changes, has a strong impact on hospitalizations. This is also shown in Figure 2E where NPIs achieving a 20% decrease in contact rate can lead to a decrease in hospitalisations comparable to yearly vaccination of the whole population. Furthermore, we find that the combined use of vaccination along NPIs should be strongly considered to limit the impact of COVID-19 on the hospital burden (Figure 2E).

These results should be taken with caution and regarded as qualitatively prospective due to the numerous sources of uncertainty (Appendix S1). In particular, comparisons should be restricted to our different scenarios that share the same core assumptions.

The sensitivity analyses (Figures S7-S10) highlight the main sources of uncertainty which correspond to factors that are difficult to predict. As discussed by Reyné et alii, 2022, the time-varying contact matrix is impossible to predict — as it depends on government policies, age-specific spontaneous behavioural changes or calendar events such as school holidays— and yet yield an huge uncertainty in the model's outputs. The seasonality also impacts strongly the results, and also unpredictable. Due to computational constraints, the sensitivity analysis did not contained the baseline contact rate even if it has a strong impact (Figure 2E). Regarding virus-related model parameters, the reduction in contagiousness due to immunity, which is difficult to estimate [Bosetti et alii, 2022; Prunas et alii, 2022], contributes to most of the variance in the model output.

Some factors are not included in the model but could affect the dynamics. For instance, this study neglects virus evolution on a long-term scale although five VOCs have already spread in France in 2021. It also neglects the potential hospitalizations attributable to patients with long-COVID.

Finally, we assumed that the intensity of non-pharmaceutical interventions will remain identical to that enforced in early spring 2022. This neglects any changes in government policies, some of which would probably be necessary to avoid hospitals saturation for some parameter sets.

This work based on empiric estimates of immune protection waning underlines the importance of combining vaccination with other type of interventions, especially NPIs such as improving indoor air quality or mask-wearing. Future work is required to identify the optimal schedule for COVID-19 vaccination campaigns as it will require narrowing many unknowns regarding the biology and spread of the virus.

References

Bosetti, Paolo et alii (Jan. 2022). "Impact of booster vaccination on the control of COVID-19 Delta wave in the context of waning immunity: application to France in the winter 2021/22". en. In: *Eurosurveillance* 27.1. Publisher: European Centre for Disease Prevention and Control, page 2101125. ISSN: 1560-7917. DOI: 10.2807/1560-7917.ES.2022.27.1.2101125. URL: https://www.eurosurveillance.org/content/10.2807/1560-7917.ES.2022.27.1.2101125 (visited on 03/17/2022).

Ghosh, Samiran, Malay Banerjee, and Vitaly Volpert (2022). "Immuno-Epidemiological Model-Based Prediction of Further Covid-19 Epidemic Outbreaks Due to Immunity Waning". en. In: *Mathematical Modelling of Natural Phenomena* 17. Publisher: EDP Sciences, page 9. ISSN: 0973-5348, 1760-6101. DOI: 10.1051/mmnp/2022017. URL: https://www.mmnp-journal.org/articles/mmnp/abs/2022/01/mmnp220088/mmnp220088.html (visited on 05/31/2022).

medRxiv preprint doi: https://doi.org/10.1101/2022.05.16.22275130; this version posted June 15, 2022. The copyright holder for this preprint (which was not certified by peer review) is the author/funder, who has granted medRxiv a license to display the preprint in perpetuity. It is made available under a CC-BY-NC 4.0 International license .

Kissler, Stephen M. et alii (May 2020). "Projecting the transmission dynamics of SARS-CoV-2 through the postpandemic period". In: *Science* 368.6493. Publisher: American Association for the Advancement of Science, pages 860–868. DOI: 10.1126/science.abb5793. URL: https://www.science.org/doi/10.1126/science.abb5793 (visited on 03/21/2022).

Ma, Yiqun et alii (June 2021). "Role of meteorological factors in the transmission of SARS-CoV-2 in the United States". en. In: *Nature Communications* 12.1, page 3602. ISSN: 2041-1723. DOI: 10.1038/s41467-021-23866-7. URL: https://www.nature.com/articles/s41467-021-23866-7 (visited on 09/25/2021).

Nyberg, Tommy et alii (2022). "Comparative Analysis of the Risks of Hospitalisation and Death Associated with SARS-CoV-2 Omicron (B.1.1.529) and Delta (B.1.617.2) Variants in England". en. In: *SSRN Electronic Journal*. ISSN: 1556-5068. DOI: 10.2139/ssrn.4025932. URL: https://www.ssrn.com/abstract=4025932 (visited on 03/15/2022).

Prunas, Ottavia et alii (Mar. 2022). "Vaccination with BNT162b2 reduces transmission of SARS-CoV-2 to household contacts in Israel". In: *Science* 375.6585. Publisher: American Association for the Advancement of Science, pages 1151–1154. DOI: 10.1126/science.abl4292. URL: https://www.science.org/doi/10.1126/science.abl4292 (visited on 03/24/2022).

Reyné, Bastien et alii (Mar. 2022). "Non-Markovian modelling highlights the importance of age structure on Covid-19 epidemiological dynamics". en. In: *Mathematical Modelling of Natural Phenomena*. Publisher: EDP Sciences. ISSN: 0973-5348, 1760-6101. DOI: 10.1051/mmnp/2022008. URL: https://www.mmnp-journal.org/articles/mmnp/abs/forth/mmnp220048/mmnp220048.html (visited on 03/15/2022).

Saad-Roy, Chadi M. et alii (Mar. 2021). "Epidemiological and evolutionary considerations of SARS-CoV-2 vaccine dosing regimes". en. In: *Science*, eabg8663. ISSN: 0036-8075, 1095-9203. DOI: 10.1126/science.abg8663. URL: https://www.sciencemag.org/lookup/doi/10.1126/science.abg8663 (visited on 03/23/2021).

Sofonea, Mircea T et alii (2022). "Analyzing and modeling the spread of SARS-CoV-2 Omicron lineages BA.1 and BA.2 in France (September 1, 2021, to February 28, 2022)". In: *Emerg Infect Dis* 28.7. DOI: 10.3201/eid2807.220033.

UKHSA (2022). "COVID-19 vaccine surveillance report - week 16". en. In: *Report*, page 22. URL: https://www.gov.uk/government/publications/covid-19-vaccine-weekly-surveillance-reports.

UKSHA (2022). "SARS-CoV-2 variants of concern and variants under investigation". en. In: page 33. URL: https://www.gov.uk/government/publications/investigation-of-sars-cov-2-variants-technical-briefings.

Acknowledgements

The authors acknowledge the ISO 9001 certified IRD i-Trop HPC (South Green Platform) at IRD Montpellier for providing HPC resources that have contributed to the research results reported within this paper. We thank all the ETE modelling team for discussions and apologize to Baptiste Elie for that reckless `rm -r *`.

Statements and Declarations

Funding : BR is funded by the Ministère de l'Enseignement Supérieur et de la Recherche.

Competing Interests : The authors have no relevant financial or non-financial interests to disclose.

Authors' Contributions : All authors contributed to the study conception and design, interpreted the results and wrote the manuscript. Analysis were performed by BR. All authors read and approved the final manuscript.

Data availability : Data and scripts will be made available in a public repository upon acceptance.

medRxiv preprint doi: https://doi.org/10.1101/2022.05.16.22275130; this version posted June 15, 2022. The copyright holder for this preprint (which was not certified by peer review) is the author/funder, who has granted medRxiv a license to display the preprint in perpetuity. It is made available under a CC-BY-NC 4.0 International license .

S1 Supplementary figures

medRxiv preprint doi: https://doi.org/10.1101/2022.05.16.22275130; this version posted June 15, 2022. The copyright holder for this preprint (which was not certified by peer review) is the author/funder, who has granted medRxiv a license to display the preprint in perpetuity. It is made available under a CC-BY-NC 4.0 International license .

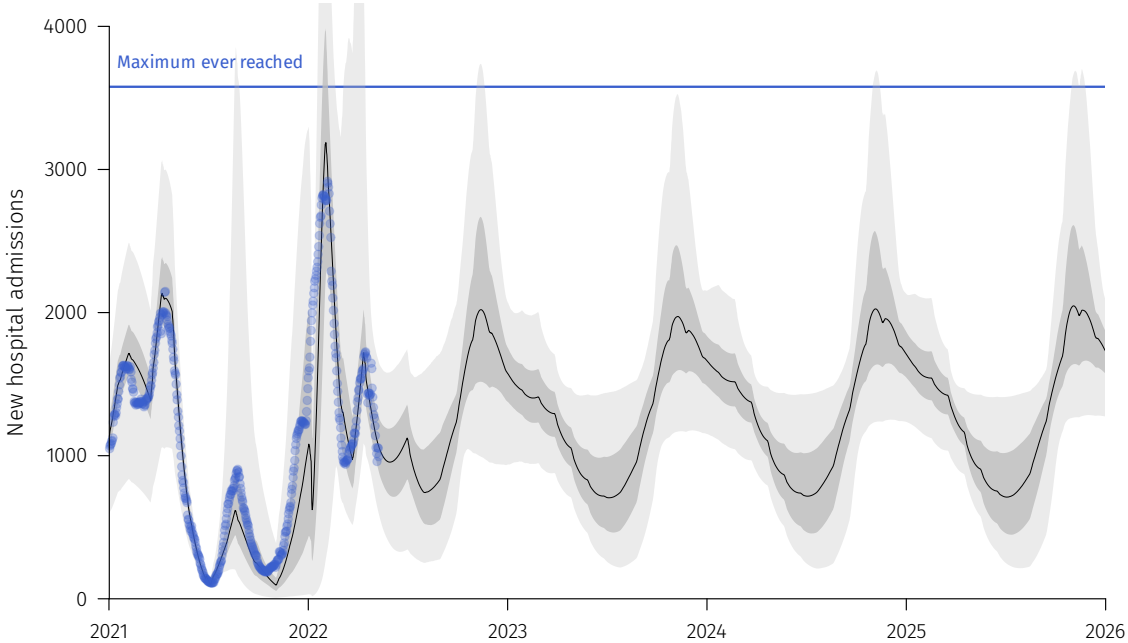

Figure S1: **Detailed output of Scenario A (no additional vaccination).** Blue dots corresponds to real data. The black line correspond to the median trajectory. Lighter shaded area correspond to the 95% confidence interval while the darker area correspond to the interquartile range. The horizontal blue line indicates the highest national incidence in hospital admissions reached during the first COVID-19 wave in France.

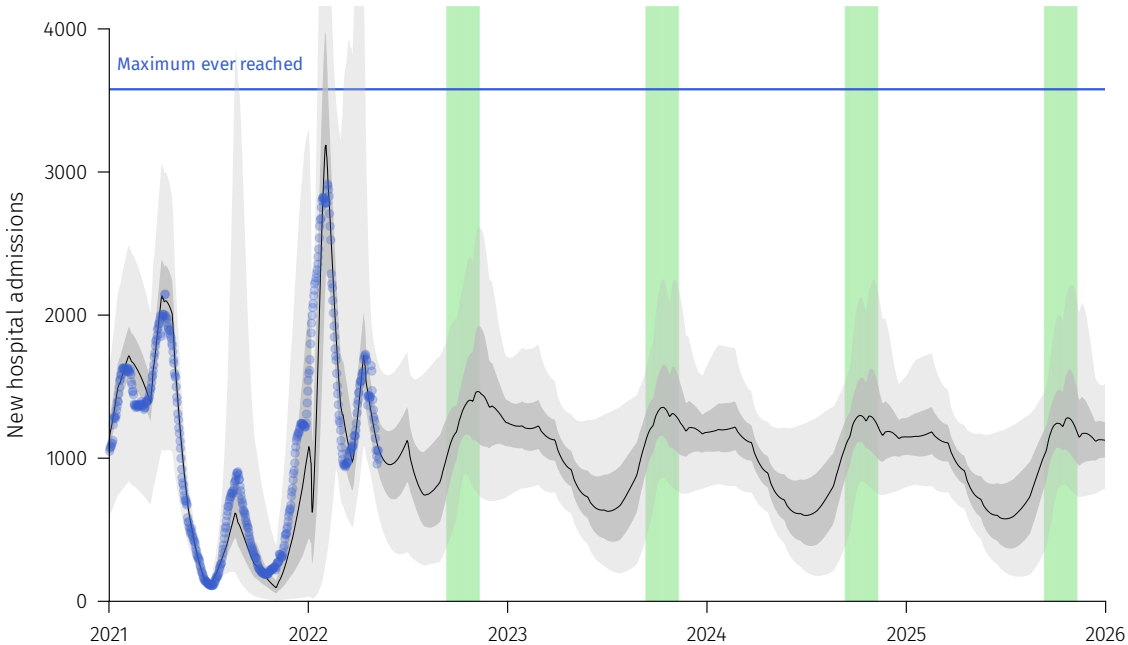

Figure S2: **Detailed output of Scenario B (yearly vaccination of individuals of more than 60 years old).** Green shaded areas correspond to vaccination campaigns periods for individuals above 60 y.o. See Figure S1 for additional details.

medRxiv preprint doi: https://doi.org/10.1101/2022.05.16.22275130; this version posted June 15, 2022. The copyright holder for this preprint (which was not certified by peer review) is the author/funder, who has granted medRxiv a license to display the preprint in perpetuity. It is made available under a CC-BY-NC 4.0 International license .

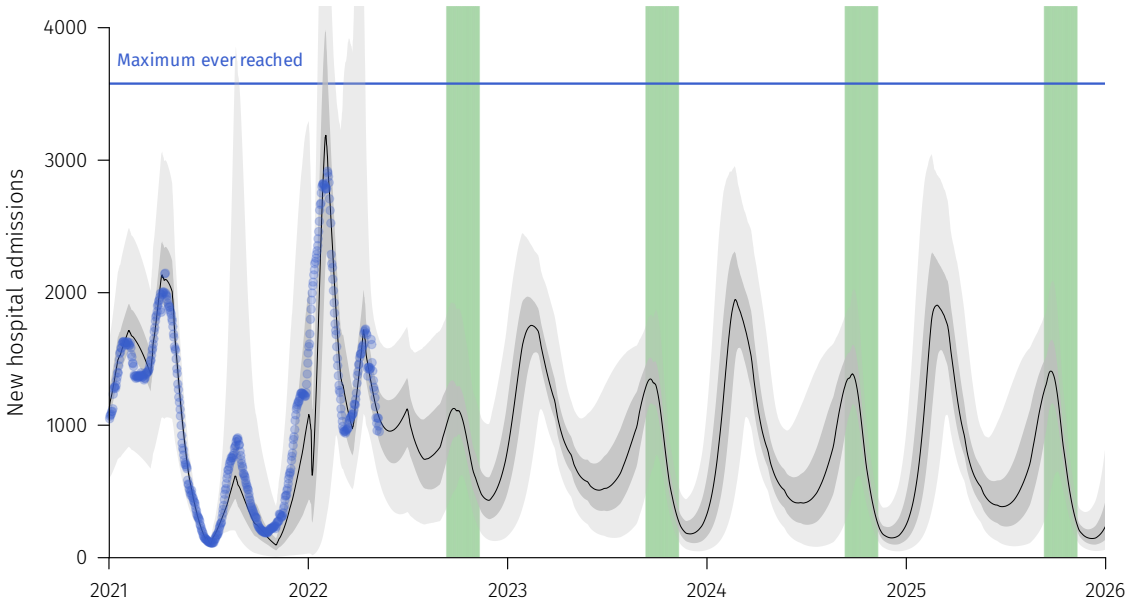

Figure S3: **Detailed output of Scenario C (yearly vaccination of all the population).** See Figure S2 for additional details.

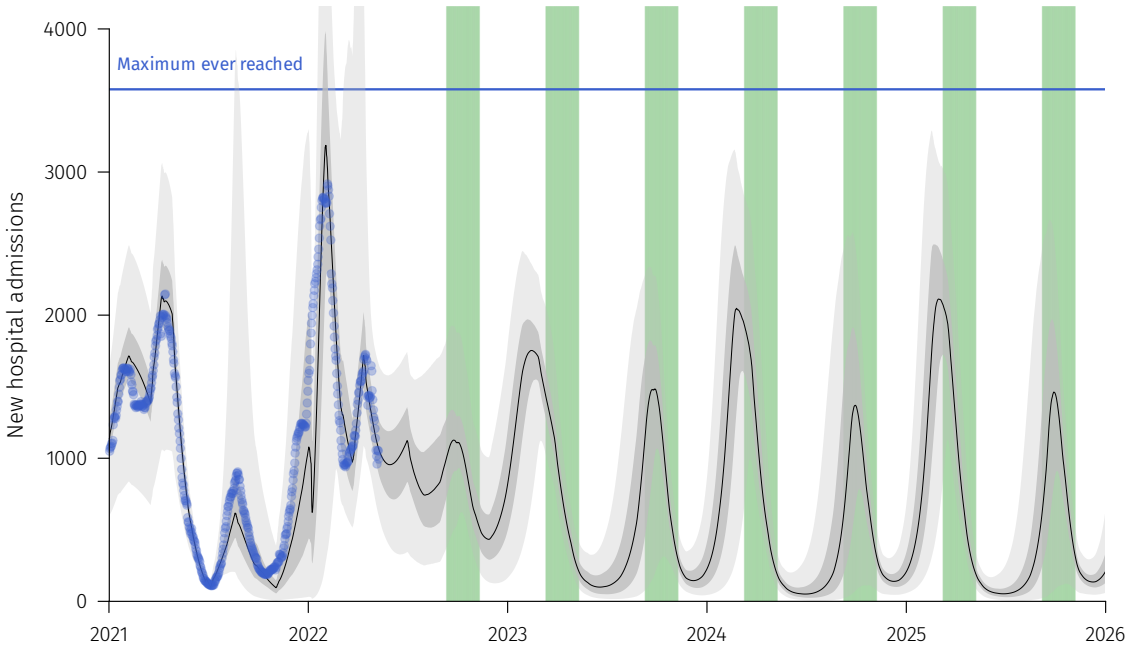

Figure S4: **Detailed output of Scenario D (vaccination of all the population twice a year).** See Figure S2 for additional details.

medRxiv preprint doi: https://doi.org/10.1101/2022.05.16.22275130; this version posted June 15, 2022. The copyright holder for this preprint (which was not certified by peer review) is the author/funder, who has granted medRxiv a license to display the preprint in perpetuity. It is made available under a CC-BY-NC 4.0 International license .

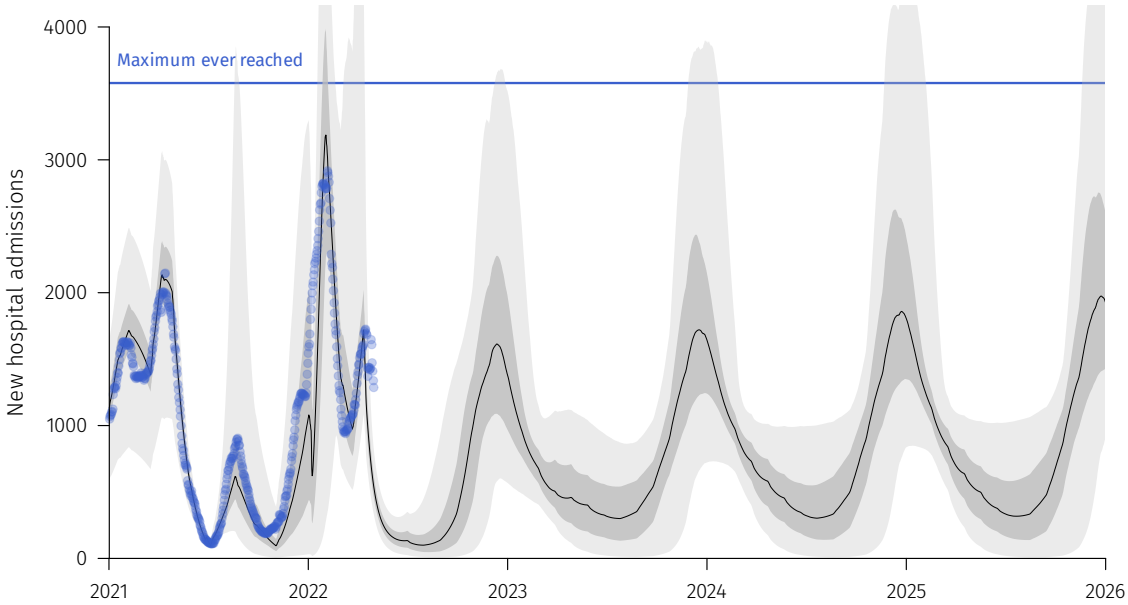

Figure S5: **Detailed output of Scenario A (yearly vaccination of all the population) with a 20% reduction of the contact rate.** See Figure S2 for additional details.

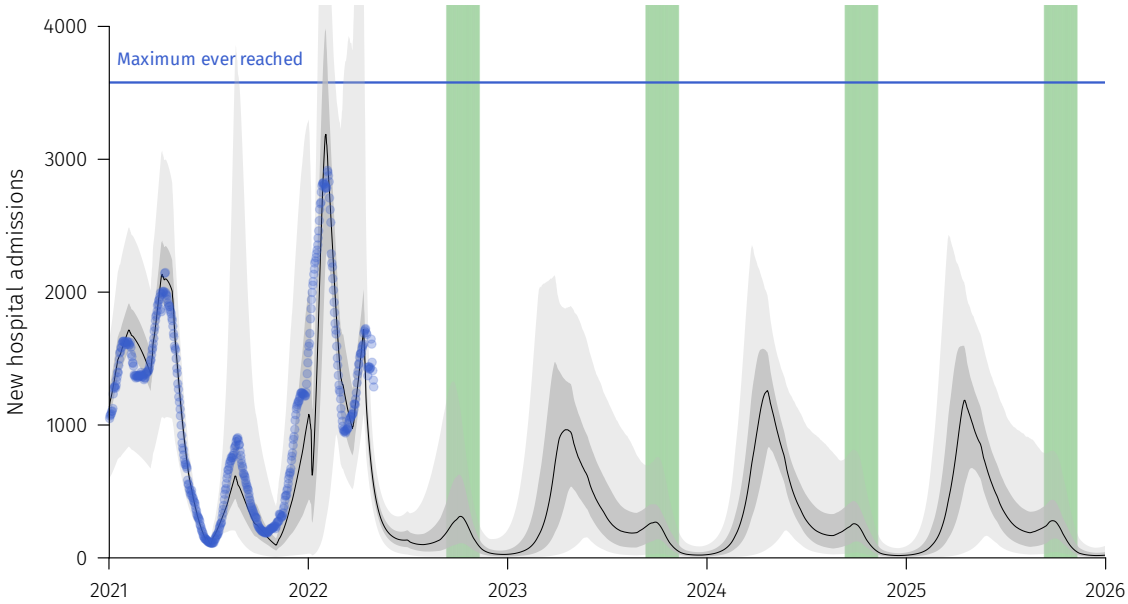

Figure S6: **Detailed output of Scenario C (yearly vaccination of all the population) with a 20% reduction of the contact rate.** See Figure S2 for additional details.

medRxiv preprint doi: https://doi.org/10.1101/2022.05.16.22275130; this version posted June 15, 2022. The copyright holder for this preprint (which was not certified by peer review) is the author/funder, who has granted medRxiv a license to display the preprint in perpetuity. It is made available under a CC-BY-NC 4.0 International license .

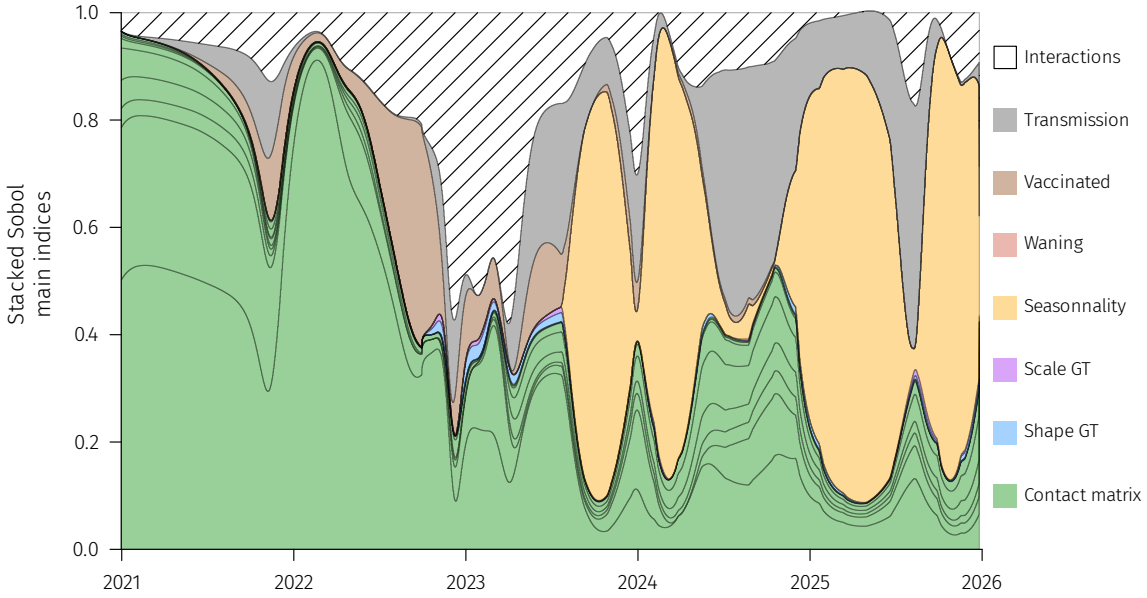

Figure S7: **Global sensitivity analysis for Scenario A.** The graphs shows the origin of the variance captured by each model parameter using Sobol indices (see Reyné et alii, 2022 for methodological details). A large part of the variations originates from the unknowns in the contact matrix between ages, as in Reyné et alii, 2022. The magnitude of seasonality also matters for the long-term trends, as well as the transmission rate (i.e. the intensity of the NPIs).

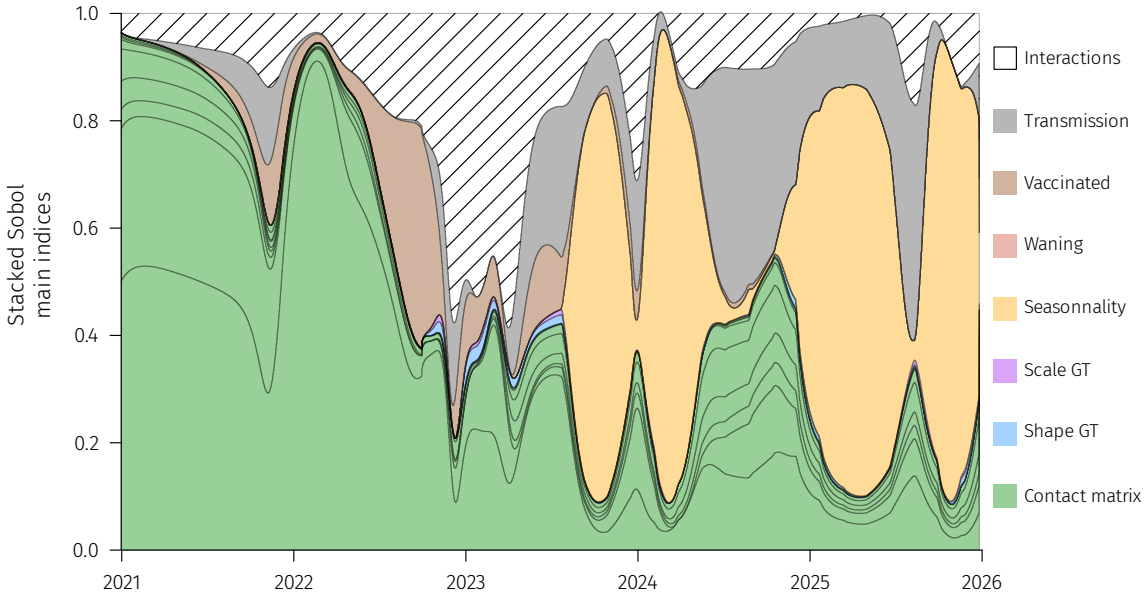

Figure S8: **Global sensitivity analysis for Scenario B.** See S7 for details.

medRxiv preprint doi: https://doi.org/10.1101/2022.05.16.22275130; this version posted June 15, 2022. The copyright holder for this preprint (which was not certified by peer review) is the author/funder, who has granted medRxiv a license to display the preprint in perpetuity. It is made available under a CC-BY-NC 4.0 International license .

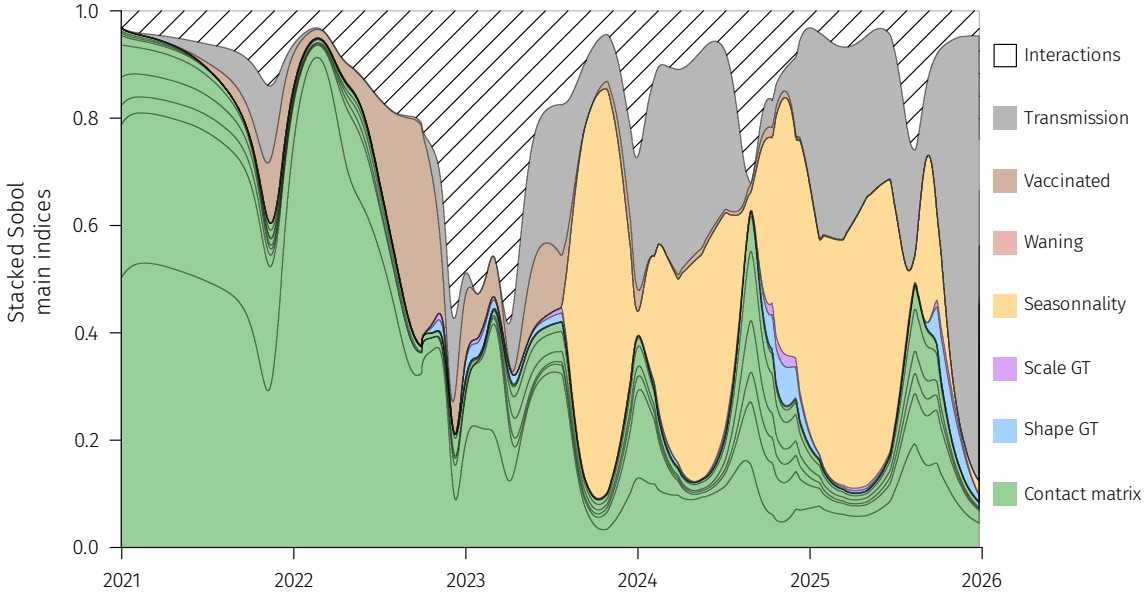

Figure S9: **Global sensitivity analysis for Scenario C.** See S7 for details.

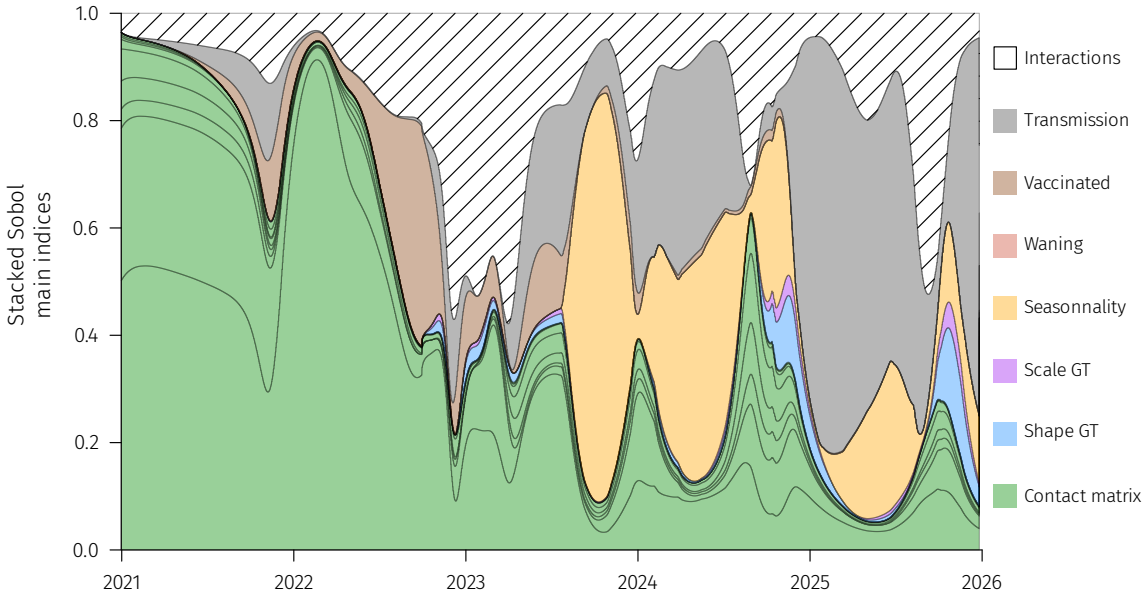

Figure S10: **Global sensitivity analysis for Scenario D.** See S7 for details.

medRxiv preprint doi: https://doi.org/10.1101/2022.05.16.22275130; this version posted June 15, 2022. The copyright holder for this preprint (which was not certified by peer review) is the author/funder, who has granted medRxiv a license to display the preprint in perpetuity. It is made available under a CC-BY-NC 4.0 International license .

S2 Model equations

The model partial differential equations system is given by:

$$\frac{\partial S(t,a)}{\partial t} = -\lambda(t,a)S(t,a) - \rho(t,a)S(t,a) \tag{S1}$$

$$\left(\frac{\partial I^m(t,a,i)}{\partial t} + \frac{\partial I^m(t,a,i)}{\partial i}\right) = -\gamma^m(a,i)I^m(t,a,i), \tag{S2}$$

$$\left(\frac{\partial I^s(t,a,i)}{\partial t} + \frac{\partial I^s(t,a,i)}{\partial i}\right) = -\gamma^s(a,i)I^s(t,a,i), \tag{S3}$$

$$\left(\frac{\partial I^d(t,a,i)}{\partial t} + \frac{\partial I^d(t,a,i)}{\partial i}\right) = -\mu(a,i)I^d(t,a,i), \tag{S4}$$

$$\left(\frac{\partial R(t,a,j)}{\partial t} + \frac{\partial R(t,a,j)}{\partial j}\right) = -\rho(t,a)R(t,a,j) - (1-\varepsilon^R(a,j))\lambda(t,a)R(t,a,j) \tag{S5}$$

$$\left(\frac{\partial V(t,a,k)}{\partial t} + \frac{\partial V(t,a,k)}{\partial k}\right) = -(1-\varepsilon^V(a,k))\lambda(t,a)V(t,a,k) - \rho^V(t,k)V(t,a,k) \tag{S6}$$

$$\left(\frac{\partial I^{mv}(t,a,i)}{\partial t} + \frac{\partial I^{mv}(t,a,i)}{\partial i}\right) = -\gamma^{mv}(a,i)I^{mv}(t,a,i), \tag{S7}$$

$$\left(\frac{\partial B(t,a,\ell)}{\partial t} + \frac{\partial B(t,a,\ell)}{\partial \ell}\right) = -(1-\varepsilon^B(a,\ell))\lambda(t,a)B(t,a,\ell) - \rho^B(t,\ell)B(t,a,\ell) \tag{S8}$$

with

$$\lambda(t,a) = \int_0^{a_{\max}} (1-c)^2 K(a,a') \int_0^{i_{\max}} \Big[\beta^m(a',i)I^m(t,a',i) + \beta^s(a',i)I^s(t,a',i) + \beta^d(a',i)I^d(t,a',i) + \beta^{mv}(a',i)(1-\xi(a'))I^{mv}(t,a',i)\Big]\,\mathrm{d}i\,\mathrm{d}a', \tag{S9}$$

for any $(t,a,i,j,k) \in \mathbb{R}^+ \times [0,a_{\max}] \times [0,i_{\max}] \times [0,j_{\max}] \times [0,k_{\max}]$.

The parameter notations are the following:

- ρ is the initial vaccination rate,
- ρ^V is the first booster dose vaccination campaign,
- ρ^B is the re-vaccination rate of prospective vaccination campaigns,
- $\gamma^{m,s}$ the recovery rates for respectively mildly and severely infected individuals,
- μ is the death rate,
- $\varepsilon^{R,V,B}$ the immunity-induced reduction of risk of infection for individuals respectively in the R, V and B compartments,
- c the intensity of NPI policy,
- $K(a,a')$ the contact matrix coefficient between age groups a and a',
- $\beta^{m,s,d,mv}$ the generation time distributions, and
- ξ the immunity-induced reduction in transmission (for 'breakthrough' infections).

medRxiv preprint doi: https://doi.org/10.1101/2022.05.16.22275130; this version posted June 15, 2022. The copyright holder for this preprint (which was not certified by peer review) is the author/funder, who has granted medRxiv a license to display the preprint in perpetuity. It is made available under a CC-BY-NC 4.0 International license .

The previous system is coupled with the following boundary conditions:

$$R(t,a,0) = \int_0^{i_{\max}} \gamma^m(a,i) I^m(t,a,i)\mathrm{d}i, \tag{S10}$$

$$V(t,a,0) = \rho(t,a)S(t,a), \tag{S11}$$

$$\begin{aligned} B(t,a,0) = \rho(t,a) \int_0^{j_{\max}} R(t,a,j)\mathrm{d}j \; + \int_0^{k_{\max}} \rho^V(t,k)V(t,a,k)\mathrm{d}k + \\ \int_0^{k_{\max}} \rho^B(t,\ell)B(t,a,\ell)\mathrm{d}\ell + \\ \int_0^{i_{\max}} \left[\gamma^{mv}(a,i)I^m v(t,a,i) + \gamma^m(a,i)I^m(t,a,i)\right]\mathrm{d}i, \end{aligned} \tag{S12}$$

$$I^m(t,a,0) = (1-p_a)\lambda(t,a)S(t,a), \tag{S13}$$

$$\begin{aligned} I^s(t,a,0) = p_a\left(1-\frac{\mathrm{ifr}_a}{p_a}\right)\lambda(t,a)\Bigg[S(t,a) + \int_0^{k_{\max}} (1-\varepsilon^V(a,k))(1-\nu^V(a,k))V(t,a,k)\mathrm{d}k \\ + \int_0^{j_{\max}} (1-\varepsilon^R(a,j)(1-\nu^R(a,j))R(t,a,j)\mathrm{d}j \\ + \int_0^{\ell_{\max}} (1-\varepsilon^B(a,\ell))(1-\nu^B(a,\ell))B(t,a,\ell)\mathrm{d}\ell\Bigg], \end{aligned} \tag{S14}$$

$$\begin{aligned} I^d(t,a,0) = \mathrm{ifr}_a\,\lambda(t,a)\Bigg[S(t,a) + \int_0^{k_{\max}} (1-\varepsilon^V(a,k))(1-\nu^V(a,k))V(t,a,k)\mathrm{d}k \\ + \int_0^{j_{\max}} (1-\varepsilon^R(a,j)(1-\nu^R(a,j))R(t,a,j)\mathrm{d}j \\ + \int_0^{\ell_{\max}} (1-\varepsilon^B(a,\ell))(1-\nu^B(a,\ell))B(t,a,\ell)\mathrm{d}\ell\Bigg], \end{aligned} \tag{S15}$$

$$\begin{aligned} I^{mv}(t,a,0) = \lambda(t,a)\Bigg[\int_0^{k_{\max}} (1-\varepsilon^V(a,k))(1-\nu^V(a,k))V(t,a,k)\mathrm{d}k \\ + \int_0^{j_{\max}} (1-\varepsilon^R(a,j)(1-\nu^R(a,j))R(t,a,j)\mathrm{d}j \\ + \int_0^{\ell_{\max}} (1-\varepsilon^B(a,\ell))(1-\nu^B(a,\ell))B(t,a,\ell)\mathrm{d}\ell\Bigg], \end{aligned} \tag{S16}$$

where

- p_a is the probability of developing a severe form,
- ifr_a is the infection fatality rate, and
- $\nu^{V,R,B}$ is the immunity-induced reduction of virulence for individuals respectively in the R, V, and B compartments.

S3 Omicron related parameters and vaccine efficacy

Regarding the omicron generation interval, we used the data provided by UKSHA [2022]. In particular, we fitted different Gamma distributions on the non-parametric data available. We tested different parameters combinations for the Gamma distribution to explore a range of generation time distributions that reflect the epidemiology of both BA.1 and BA.2 variants. In Figure S11, we show a subset of these Gamma distributions explored within the sensitivity analysis.

medRxiv preprint doi: https://doi.org/10.1101/2022.05.16.22275130; this version posted June 15, 2022. The copyright holder for this preprint (which was not certified by peer review) is the author/funder, who has granted medRxiv a license to display the preprint in perpetuity. It is made available under a CC-BY-NC 4.0 International license .

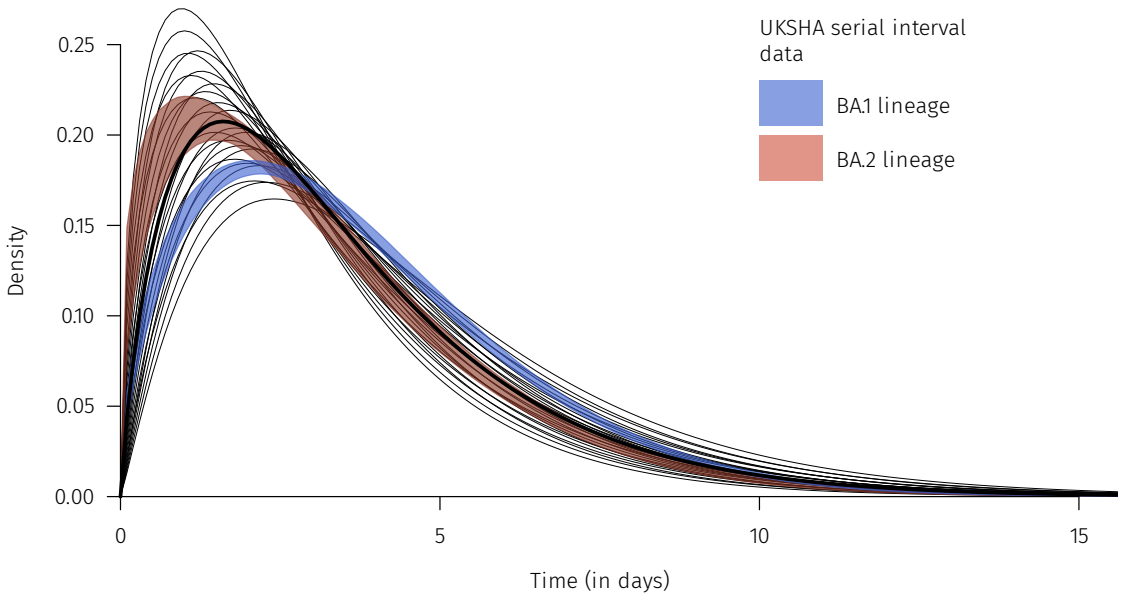

Figure S11: **Omicron generation time.** Shaded areas data originate from the UKSHA [2022] report. The lines correspond to a subset of the Gamma distributions used in the sensitivity analysis. The thicker line corresponds to the baseline Gamma distribution.

Regarding the parameterisation of vaccine effectiveness, we used data provided by the UKHSA [2022] report (`https://assets.publishing.service.gov.uk/government/uploads/system/uploads/attachment_data/file/1070356/Vaccine-surveillance-report-week-16.pdf`). The raw data was not available so we used the online tool WebPlot Digitalizer (`https://apps.automeris.io/wpd/`) to retrieve the values. For simplicity, we assumed that individuals received the Pfizer/BioNTech (BNT162b2) vaccine, which was the most widespread in France. We fitted linear models on vaccine effectiveness against symptomatic disease and hospital admissions for the Delta and Omicron VOC. Note that the intrinsic virulence of Omicron is assumed to be divided by 3 (parameter p_a in the model) compared to Delta following UK data Nyberg et alii, 2022.

In the sensitivity analysis, we included variations in vaccine protection against symptomatic disease and against hospitalization risk. We used the linear model best fit as our baseline and generated variation by applying a coefficient to the intercept spanning from -0.05 to 0.05 (Figure 1B).

The reduction of transmission (in so-called 'breakthrough' infections) was assumed to be of 50% for vaccinated individuals, as in others modelling works [Bosetti et alii, 2022]. This reduction in transmission was also applied to recovered people that got reinfected.

For the other model parameters, they are identical to Reyné et alii [2022].